Pergamon

Int. J. Engng Sci. Vol. 34, No. 15, pp. 1705–1716, 1996

PII: S0020-7225(96)00055-9
0020-7225/96 $15.00 + 0.00

INTERFACE CRACKING BETWEEN FUNCTIONALLY GRADED COATINGS AND A SUBSTRATE UNDER ANTIPLANE SHEAR

Z.-H. JIN and R. C. BATRA

Department of Engineering Science and Mechanics, Virginia Polytechnic Institute and State University, Blacksburg, VA 24061-0219, U.S.A.

Abstract—Coating technology plays a significant role in a number of applications such as high temperatures, corrosion, oxidation, wear, and interface. In this paper, we investigate the interface cracking between ceramic and/or functionally graded coatings (FGM coatings) and a substrate under antiplane shear. Four coating models are considered, namely single layered homogeneous coating, double layered piece-wise homogeneous coating, single layered FGM coating and double layered coating with an FGM bottom coat. Mode III stress intensity factors (SIFs) are calculated for the different coating models. In the case of $\mu_L > \mu_0$, where μ_0 is the shear modulus of the substrate and μ_L the shear modulus of the material at the surface of the coating, it is found that the single layered FGM coating reduces SIF slightly, whereas the coating system with a top homogeneous layer and a thin FGM bottom layer reduces SIF significantly. In the case of $\mu_L < \mu_0$, the SIF is found to be larger for the FGM coatings than for the homogeneous coatings. The FGM coating, however, may still be superior to homogeneous coatings in this case as FGM coatings usually provide better bonding strength between the coating and substrate. Finally, the applicability of the SIF concept in the fracture of FGM coatings is discussed. Large modulus gradients in thin coatings may seriously restrict the application of SIFs as the SIF-dominant zone may fall into the crack tip nonlinear deformation and damage zone. The same argument exists for some interphase models in interface crack solutions.

1. INTRODUCTION

Coating technology plays an important role in a number of applications, including high temperatures, corrosion, oxidation, wear, and interface. High temperature resistant ceramic thermal barrier coatings used for engine applications improve turbine efficiency, component durability and fuel economy [1,2]. Cutting tools coated with wear resistant ceramic layers have higher cutting performance and longer life [3,4]. Conventional coatings usually consist of a single or double layered piece-wise homogeneous coat deposited on a substrate. These coatings are usually susceptible to cracking due to their low fracture toughness. Thermal residual stresses due to the mismatch of material properties develop at the coating–substrate interfaces. For example, surface cracking and interface debonding occurred when a ceramic-coating/metal-substrate system was subjected to thermal shocks [5,6]. In order to overcome these disadvantages of conventional coatings, multilayer coatings, and (especially) functionally graded coatings (FGM coating) have been developed. In an FGM coating, the compositions and microstructures are continuously varied in the thickness direction and the mismatch of material properties at the coating substrate interface is eliminated [7]. This enhances the bonding strength, reduces the thermal residual stresses, and significantly improves the fracture toughness and strength of the coating. Experimental results [5,6] show that the coating damage in the form of surface and interface cracking in a system of ceramic-coating/metal-substrate under thermal shocks is significantly reduced by replacing the ceramic coating with a ceramic-metal graded coating.

Erdogan [8] has discussed a number of aspects of fracture mechanics of FGMs. Jin and Noda [9] showed that the crack tip fields in general nonhomogeneous materials are identical to those in homogeneous materials as long as the material properties are continuous and piece-wise continuously differentiable. Jin and Batra [10] studied the fracture toughness and residual strength of an FGM; several investigators (see e.g. [11–17]), have calculated stress intensity factors in nonhomogeneous

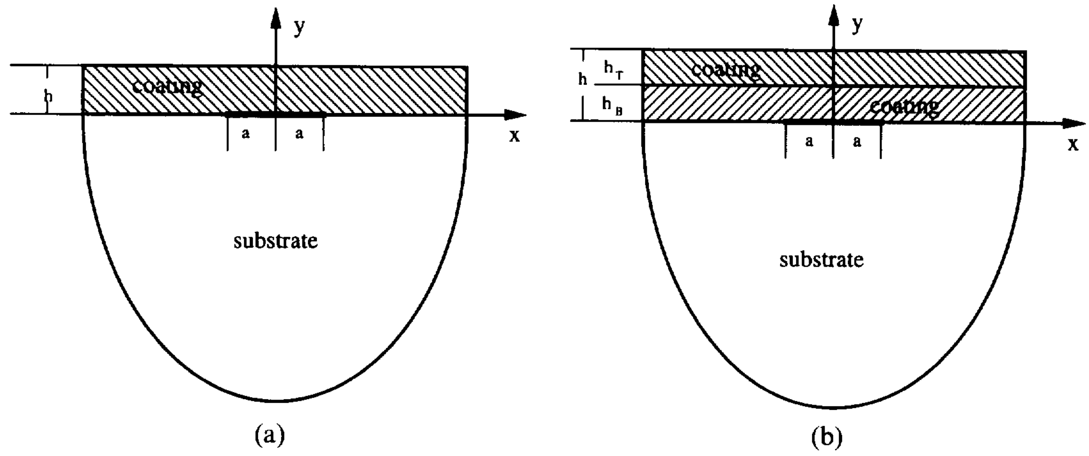

Fig. 1. (a) Single layered coating on a substrate with an interface crack. (b) Double layered coating on a substrate with an interface crack between the coating and substrate.

materials. Bao and Wang [18] have studied multiple surface cracking in an FGM coating using a finite element method. Erdogan and Ozturk [19] considered periodic surface cracking in an FGM coating under antiplane shear. In this paper, we investigate the interface cracking between ceramic and/or FGM coatings and a substrate under antiplane shear. Four coating models are considered, namely: single layered homogeneous coating, double layered piece-wise homogeneous coating, single layered FGM coating and double layered coating with an FGM bottom coat. The effect of the coating forms on the stress intensity factor is discussed. The influence of the modulus gradients in the FGM coatings on the size of the stress-intensity-factor dominant zone is also studied.

2. COATING MODELS

Coatings are usually very thin compared with the substrate. We consider a semi-infinite substrate bonded with a coating of thickness h at its surface (Fig. 1). The coating–substrate system is subjected to antiplane shear at the coating surface. The rectangular Cartesian coordinates (x, y) are selected so that the x-axis is along the coating–substrate interface and the y-axis normal to it as shown in Fig. 1.

Four coating models are considered in the present study. The first is a single layered homogeneous coating with the shear modulus μ_L; the shear modulus of the substrate is μ_0. In a ceramic-coating/metal-substrate system, μ_L is usually higher than μ_0. The second model is a single layered FGM coating with the shear modulus assumed to vary continuously from μ_0 at the interface ($y = 0$) to μ_L at the surface of the coating ($y = h$) and is given by

$$\mu = \mu_0 e^{\beta(y/h)} \tag{1}$$

where

$$\beta = \ln\frac{\mu_L}{\mu_0} \tag{2}$$

is a nondimensional constant describing the gradient of the shear modulus and can be related to the volume fractions of the constituents of the coating. The third model is a double layered coating with an FGM bottom coat. The shear modulus is assumed to be continuous and is given by

$$\mu = \mu_0 e^{\beta(y/h_B)}, \qquad 0 \le y \le h_B \tag{3a}$$

$$\mu = \mu_L, \qquad h_B \le y \le h \tag{3b}$$

$$\beta = \ln\frac{\mu_L}{\mu_0} \tag{3c}$$

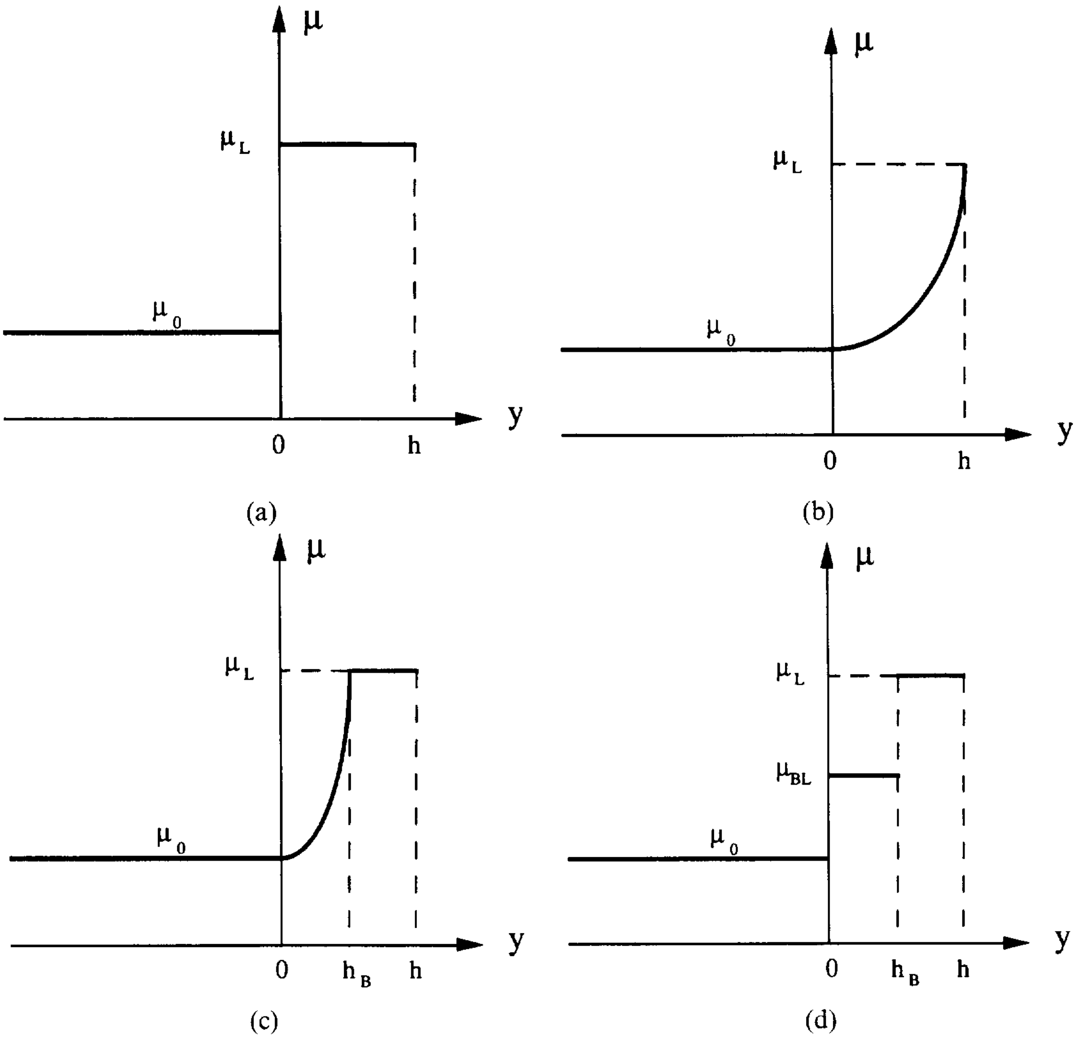

Fig. 2. Variation of shear modulus through the thickness for (a) a single layered homogeneous coating on a substrate; (b) a single layered FGM coating on a substrate; (c) a double layered coating with an FGM bottom coat on a substrate; (d) a double layered piece-wise homogeneous coating on a substrate.

where h_B is the thickness of the bottom FGM layer [Fig. 1(b)]. The fourth model is a double layered coating with piece-wise homogeneous layers. The shear moduli of the top and bottom layers are μ_L and μ_{BL}, respectively. The variations of the shear modulus through the thickness of the coating for the four models are shown in Fig. 2.

3. AN INTERFACE CRACK BETWEEN THE COATING AND SUBSTRATE

To evaluate the effect of modulus gradients on the interface cracking between the coating and substrate, we study the stress intensity factors at the tip of a mode III interface crack of length $2a$ (cf. Fig. 1) for the above stated four coating models. The basic elasticity equations for nonhomogeneous materials undergoing antiplane shear deformations are

$$\frac{\partial}{\partial x}\left(\mu\frac{\partial w}{\partial x}\right)+\frac{\partial}{\partial y}\left(\mu\frac{\partial w}{\partial y}\right)=0 \tag{4}$$

$$\left(\tau_x, \tau_y\right) = \mu(x, y)\left(\frac{\partial w}{\partial x}, \frac{\partial w}{\partial y}\right) \tag{5}$$

where w is the antiplane displacement, (τ_x, τ_y) are the shear stresses and $\mu(x, y)$ is the shear modulus.

The governing equations for the four different coatings are as follows. For the single layered homogeneous model:

$$\nabla^2 w = 0 \tag{6a}$$

$$(\tau_x, \tau_y) = \mu_L\left(\frac{\partial w}{\partial x}, \frac{\partial w}{\partial y}\right). \tag{6b}$$

For the single layered FGM model:

$$\nabla^2 w + \frac{\beta}{h}\frac{\partial w}{\partial y} = 0 \tag{7a}$$

$$(\tau_x, \tau_y) = \mu_0 e^{\beta(y/h)}\left(\frac{\partial w}{\partial x}, \frac{\partial w}{\partial y}\right). \tag{7b}$$

For the double layered coating with an FGM bottom coat:

$$\nabla^2 w + \frac{\beta}{h_B}\frac{\partial w}{\partial y} = 0, \qquad 0 < y < h_B \tag{8a}$$

$$\nabla^2 w = 0, \qquad h_B < y < h \tag{8b}$$

$$(\tau_x, \tau_y) = \mu_0 e^{\beta(y/h_B)}\left(\frac{\partial w}{\partial x}, \frac{\partial w}{\partial y}\right), \qquad 0 < y < h_B \tag{8c}$$

$$(\tau_x, \tau_y) = \mu_L\left(\frac{\partial w}{\partial x}, \frac{\partial w}{\partial y}\right), \qquad h_B < y < h. \tag{8d}$$

Finally, for the double layered piece-wise homogeneous coating:

$$\nabla^2 w = 0 \tag{9a}$$

$$(\tau_x, \tau_y) = \mu_{BL}\left(\frac{\partial w}{\partial x}, \frac{\partial w}{\partial y}\right), \qquad 0 < y < h_B \tag{9b}$$

$$(\tau_x, \tau_y) = \mu_L\left(\frac{\partial w}{\partial x}, \frac{\partial w}{\partial y}\right), \qquad h_B < y < h. \tag{9c}$$

The boundary condition at the coating surface is taken as

$$\tau_y = \tau_0, \quad |x| < \infty, \quad y = h. \tag{10}$$

At the interface between the coating and substrate, we have

$$\tau_y = 0, \quad |x| \le a, \quad y = 0^{\pm} \tag{11a}$$

$$[w] = 0, \; [\tau_y] = 0, \; |x| \ge a, \; y = 0 \tag{11b,c}$$

where $[f]$ equals the jump in the value of f across the interface. For the double layered coatings, we also require that the shear stress τ_y and the displacement w be continuous across the interface between the two layers.

By using the integral transform the above boundary value problem for each one of the four coating models can be reduced to the following singular integral equation:

$$\int_{-1}^{1}\left[\frac{1}{t-s} + K(s, t)\right]\phi(t)\mathrm{d}t = -2\pi, \quad |s| \le 1 \tag{12}$$

where $\phi(t)$, the normalized dislocation density function along the crack face, is given by

$$\phi(x) = \left.\frac{\partial[w]}{\partial x}\right|_{y=0} \tag{13}$$

and satisfies

$$\int_{-1}^{1} \phi(t)\mathrm{d}t = 0. \tag{14}$$

In equation (12), the nondimensional variables t and s are defined as

$$(t, s) = (x, x')/a \tag{15}$$

and $K(s, t)$ is a Fredholm kernel given by

$$K(s, t) = \int_{0}^{\infty} F_i(\xi) \sin[(s - t)\xi] \,\mathrm{d}\xi, \quad i = 1, 2, 3, 4 \tag{16}$$

in which functions $F_i(\xi)$ are as follows. For the single layered homogeneous coating:

$$F_1(\xi) = 1 - \frac{(1 + \mu_0/\mu_L)(1 - \mathrm{e}^{-2\frac{h}{a}\xi})}{1 - \mathrm{e}^{-2\frac{h}{a}\xi} + \frac{\mu_0}{\mu_L}(1 + \mathrm{e}^{-2\frac{h}{a}\xi})}. \tag{17}$$

For the single layered FGM model:

$$F_2(\xi) = 1 - \frac{2(1 - \mathrm{e}^{-\alpha})}{1 - \mathrm{e}^{-\alpha} + 2\left(\frac{h}{a}\right)\xi\left(\frac{1}{\alpha+\beta} + \frac{\mathrm{e}^{-\alpha}}{\alpha-\beta}\right)} \tag{18a}$$

$$\alpha(\xi) = \sqrt{\beta^2 + 4\left(\frac{h}{a}\right)^2 \xi^2}. \tag{18b}$$

For the double layered coating with an FGM bottom coat:

$$F_3(\xi) = 1 - \frac{2}{1 + \frac{2(h_B/a)\xi(H_1 + H_2\mathrm{e}^{-\alpha_B})}{(\beta+\alpha_B)H_1 + (\beta-\alpha_B)H_2\mathrm{e}^{-\alpha_B}}} \tag{19a}$$

$$\alpha_B(\xi) = \sqrt{\beta^2 + 4\left(\frac{h_B}{a}\right)^2 \xi^2} \tag{19b}$$

$$H_1 = (\beta - \alpha_B)\left(1 + \mathrm{e}^{-2\frac{h_T}{a}\xi}\right) - 2\frac{h_B}{a}\xi\left(1 - \mathrm{e}^{-2\frac{h_T}{a}\xi}\right) \tag{19c}$$

$$H_2 = -(\beta + \alpha_B)(1 + \mathrm{e}^{-2\frac{h_T}{a}\xi}) + 2\frac{h_B}{a}\xi\left(1 - \mathrm{e}^{-2\frac{h_T}{a}\xi}\right), \tag{19d}$$

where h_T is the thickness of the top homogeneous layer and $h = h_T + h_B$. Finally, for the double layered piece-wise homogeneous coating:

$$F_4(\xi) = 1 - \frac{1 + (\mu_0/\mu_{BL})H(\xi)}{H(\xi) + \mu_0/\mu_{BL}} \tag{20a}$$

$$H(\xi) = \frac{(\mu_L/\mu_{BL} + 1)\left(1 - \mathrm{e}^{-2\frac{h}{a}\xi}\right) - (\mu_L/\mu_{BL} - 1)\left(\mathrm{e}^{-2\frac{h_T}{a}\xi} - \mathrm{e}^{-2\frac{h_B}{a}\xi}\right)}{(\mu_L/\mu_{BL} + 1)\left(1 + \mathrm{e}^{-2\frac{h}{a}\xi}\right) - (\mu_L/\mu_{BL} - 1)\left(\mathrm{e}^{-2\frac{h_T}{a}\xi} + \mathrm{e}^{-2\frac{h_B}{a}\xi}\right)}. \tag{20b}$$

According to the singular integral equation method [20,21], equation (12) has a solution of the form

$$\phi(t) = \frac{\psi(t)}{\sqrt{1 - t^2}}, \quad |t| \le 1 \tag{21}$$

where $\psi(t)$ is a continuous and bounded function on the interval $[-1, 1]$.

The shear stress τ_y at the interface just ahead of the crack tip $(x > a,\ y = 0)$ for every coating is evaluated as

$$\tau_y\big|_{y=0} = \tau_0 + \frac{\tau_0}{2\pi}\int_{-1}^{1}\left[\frac{1}{t - s} + K(s, t)\right]\phi(t)\mathrm{d}t. \tag{22}$$

The mode III stress intensity factor K_{III} is defined by

$$K_{III} = \lim_{x \to a^+} \sqrt{2\pi(x-a)}\tau_y\,|_{y=0} \tag{23}$$

and is normalized as

$$K^* = \frac{K_{III}}{\tau_0\sqrt{\pi a}} = -\frac{1}{2}\psi(1). \tag{24}$$

4. EFFECT OF THE MODULUS GRADIENTS ON THE APPLICABILITY OF STRESS INTENSITY FACTORS

It is known [9,13,14] that for nonhomogeneous materials, the elastic crack tip fields are identical to those in homogeneous materials if the material properties are continuous and piece-wise continuously differentiable. Hence, the stress intensity factor (SIF) concept may still be used to study the fracture behavior of nonhomogeneous materials including FGMs and FGM coatings. While the gradients of the elasticity modulus do not influence the crack tip singular property of stress fields, they may affect the size of the region dominated by the square root singular solutions. As a result, the applicability of SIFs may also be affected. A rough estimate of this effect was made in [10] under plane strain conditions. Assuming that the stress state is controlled by the SIF at points a distance r from the crack tip, then the gradients of Young's modulus at those points should satisfy

$$\frac{1}{E}\left|\frac{\partial E}{\partial x_\alpha}\right| \ll \frac{1}{r}, \quad \frac{1}{E}\left|\frac{\partial^2 E}{\partial x_\alpha \partial x_\beta}\right| \ll \frac{1}{r^2}. \tag{25}$$

For antiplane shear, equation (25) is equivalent to

$$\frac{1}{\mu}\left|\frac{\partial \mu}{\partial x}\right| \ll \frac{1}{r}, \quad \frac{1}{\mu}\left|\frac{\partial \mu}{\partial y}\right| \ll \frac{1}{r}. \tag{26}$$

For the coating problems considered here, it reduces to

$$r \ln\frac{\mu_L}{\mu_0} \ll h \tag{27}$$

for the single layered FGM coating, and

$$r \ln\frac{\mu_L}{\mu_0} \ll h_B \tag{28}$$

for the double layered coating with an FGM bottom coat. Since the square root singular crack tip solutions are expected to be valid only at $r \ll a$ and $r \ll h$ (or h_B), it seems from conditions (27) and (28) that the modulus gradients (described by the ratio μ_L/μ_0 and the thickness h or h_B) in the coatings do not require additional conditions on the size of the SIF-dominant zone (usually referred to as K-dominant zone) provided that $\ln(\mu_L/\mu_0)$ is of order unity. However, the size of the K-dominant zone will decrease with increasing shear modulus ratio μ_L/μ_0 for a fixed coating thickness and the zone may fall into the crack tip nonlinear deformation and damage zone for very large μ_L/μ_0. As a result, the SIF will lose its meaning as a controlling parameter for the stress state at the crack tip.

The same argument may be made for some interphase models in interface crack problems [15,22–24] when the thickness of the interphase layer between two dissimilar materials is very small. In particular, the crack tip solutions of the standard interface crack problem with ideal sharp interface may not be recovered by taking the limit $h \to 0$ (h equals the thickness of the interphase layer) in the solution of the interphase models under antiplane shear conditions. The K-dominant zone will shrink to the crack tip in this limiting process. In fact, the mode III SIF for an interphase model of Ozturk and Erdogan [15] did not approach the value of the corresponding standard interface crack when the thickness of the interphase layer became vanishingly small.

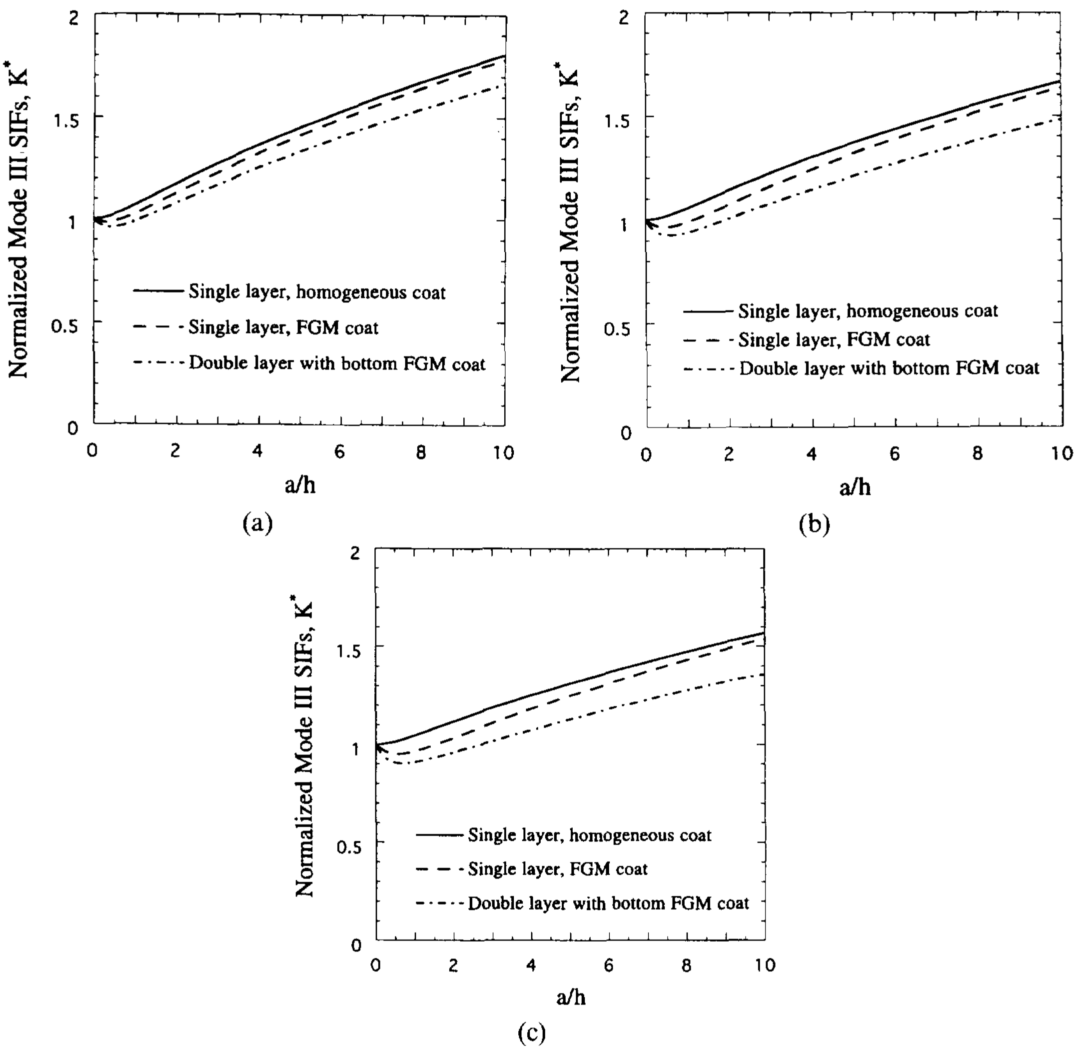

Fig. 3. Nondimensional SIF versus the normalized half crack length a/h, for (a) $\mu_L/\mu_0 = 2$; (b) $\mu_L/\mu_0 = 3$; (c) $\mu_L/\mu_0 = 4$.

5. NUMERICAL RESULTS AND DISCUSSION

In high temperature applications, the coatings are generally made from ceramics and their moduli are usually higher than that of the metal substrate. In some cutting tool applications, the modulus of a coating may be lower than that of the substrate (for example, for alumina-coated tungsten carbide). We will consider both cases: $\mu_L > \mu_0$ and $\mu_L < \mu_0$ in equations (1)–(3). Figure 3(a) shows the nondimensional stress intensity factor (SIF) K^*, versus the normalized half crack length a/h for the single layered homogeneous coating (SLHC), the single layered FGM coating (SLFC) and the double layered coating with an FGM bottom coat (DLFBC). In the DLFBC case, the thicknesses of the top and bottom layers are both taken as half of the total thickness, i.e. $h_T = h_B = h/2$ in equation (19). The shear modulus ratio μ_L/μ_0 is taken as 2. It is seen from the figure that when the crack length is very small compared with the coating thickness ($a/h \ll 1$), the normalized SIFs tend to unity for SLHC, SLFC and DLFBC coatings. When the crack length becomes larger, the SIFs decrease a little at first and then increase. The SIF of SLFC is slightly lower than that of SLHC especially for longer cracks. The SIF for DLFBC is always lower than that of SLHC and SLFC. Hence, in terms of SIF reduction, DLFBC is a better alternative to the conventional SLHC. Figure 3(b) and (c) show similar results for $\mu_L/\mu_0 = 3$ and 4.

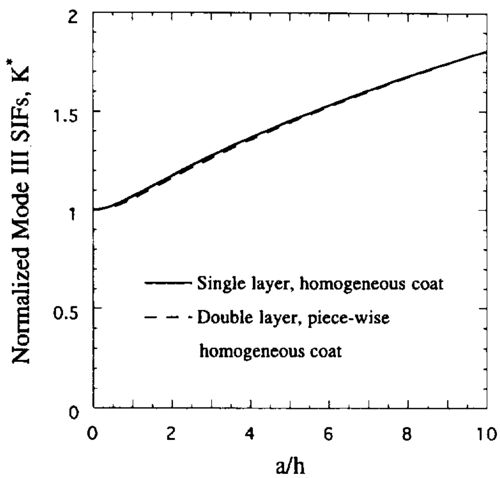

Fig. 4. Nondimensional SIF versus the normalized half crack length a/h, for a double layered piece-wise homogeneous coating ($\mu_L/\mu_0 = 2$).

Figure 4 shows the variation of SIF with a/h for double layered piece-wise homogeneous coating (DLHC) with $\mu_L/\mu_0 = 2$ and $\mu_{BL}/\mu_0 = 1.5$. It is observed that the SIFs for DLHC and SLHC are essentially the same. Similar results are obtained for $\mu_L/\mu_0 > 1$ and $1 < \mu_{BL}/\mu_0 < \mu_L/\mu_0$.

In order to evaluate the effect of the thickness of the FGM layer in DLFBC, the SIFs versus a/h for DLFBC with $h_T/h = 0.1$, 0.5 and 0.9 are depicted in Fig. 5(a)–(c). It is seen that the SIF decreases with a decrease in the thickness of the FGM layer (an increase in h_T/h). These theoretical results suggest that a better coating is obtained by introducing an FGM bonding coat between a substrate and a top homogeneous layer. The coating system thus obtained has reduced interface stress intensity factors and improved bonding strength.

For $\mu_L/\mu_0 < 1$, i.e. the modulus of the coating is lower than that of the substrate, the SIF is found to be higher for the FGM coatings than for homogeneous coatings. Figure 6 shows results for $\mu_L/\mu_0 = 0.5$. The FGM coatings may still be superior to homogeneous coatings as they usually provide better bonding strength between the coating and substrate, reduced thermal residual stresses, and higher fracture toughness and strength.

In order to study the effect of the modulus gradient on the K-dominant zone size, we evaluate the shear stress τ_y at the crack extension line ($x > a$, $y = 0$). The total stress is given by equation (22) and the inverse-square-root solution at the crack tip is

$$\tau_y^K = \frac{K_{\rm III}}{\sqrt{2\pi(x-a)}} = \tau_0\sqrt{\frac{a}{2r}}\left[-\frac{1}{2}\psi(1)\right] \tag{29}$$

where $r = x - a$ is the distance from the crack tip. The ratio of τ_y^K to τ_y is

$$R_s = \left.\frac{\tau_y^K}{\tau_y}\right|_{y=0} = \sqrt{\frac{a}{2r}}\left[-\frac{1}{2}\psi(1)\right] \bigg/ \left\{1 + \frac{1}{2\pi}\int_{-1}^{1}\left[\frac{1}{t-s} + K(s,t)\right]\phi(t)\mathrm{d}t\right\}. \tag{30}$$

The region where the stress ratio R_s satisfies

$$0.9 \le R_s \le 1.1 \tag{31}$$

may be regarded as the K-dominant zone.

Figure 7(a) shows the stress ratio R_s versus the normalized distance, $r/h = (x-a)/h$, from the crack tip for the single layered FGM coating when $h/a = 1.0$. It is evident that the size of the K-dominant zone along the crack extension line is $0.11h \sim 0.12h$ for $\mu_L/\mu_0 = 2$, $0.08h \sim 0.09h$ for $\mu_L/\mu_0 = 4$ and $0.06h \sim 0.07h$ for $\mu_L/\mu_0 = 8$. Hence, the size of the K-dominant zone decreases with an increase in the shear modulus ratio μ_L/μ_0, or equivalently, the gradient of the modulus since the gradient normalized by the modulus is $(1/h)\ln(\mu_L/\mu_0)$. The K-dominant zone may fall

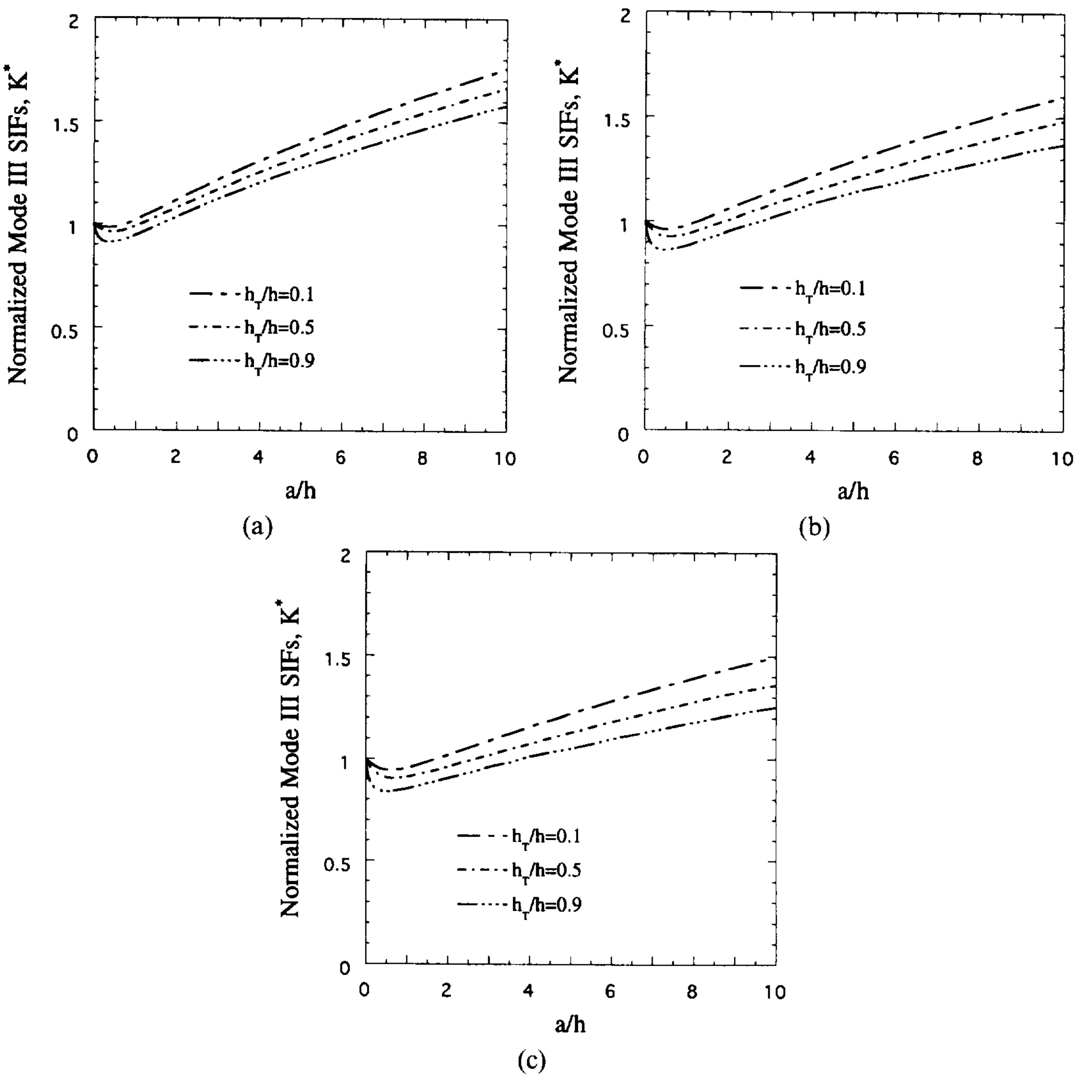

Fig. 5. Nondimensional SIF versus the normalized half crack length a/h, for the double layered coating with an FGM bottom coat: (a) $\mu_L/\mu_0 = 2$; (b) $\mu_L/\mu_0 = 3$; (c) $\mu_L/\mu_0 = 4$.

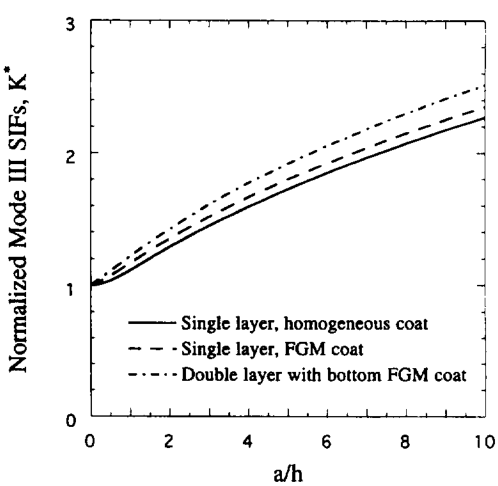

Fig. 6. Nondimensional SIF versus the normalized half crack length a/h, ($\mu_L/\mu_0 = 0.5$).

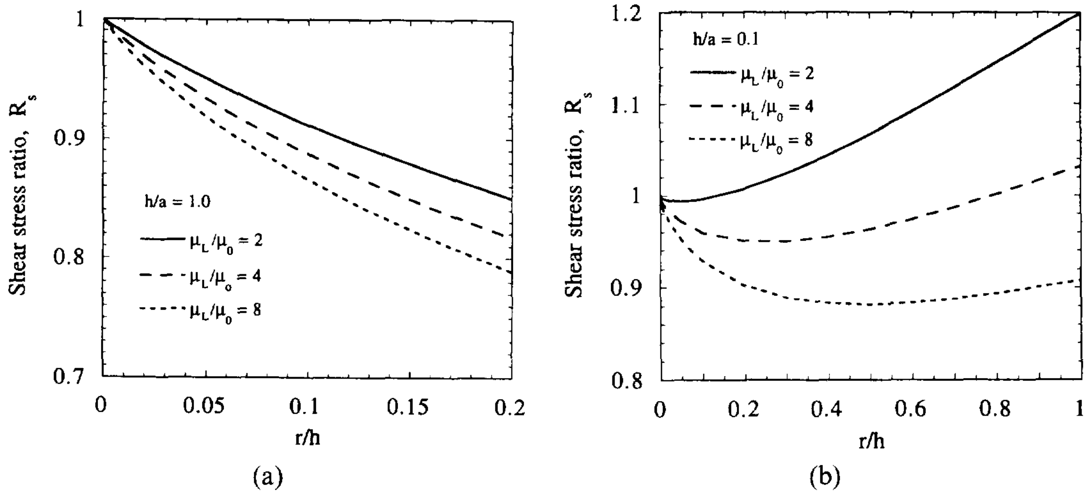

Fig. 7. The square-root singular stress divided by the total stress, $R_s = \tau_y^K/\tau_y$, at the crack extension line ($r = x-a > 0$, $y = 0$) for a single layered FGM coating: (a) $h/a = 1.0$; (b) $h/a = 0.1$.

into the crack tip nonlinear deformation and damage zone for thin FGM coatings if μ_L/μ_0 is very large. In that case, the SIF cannot be justified as a controlling parameter of the stress state at the crack tip. Figure 7(b) shows results for $h/a = 0.1$. The size of the K-dominant zone is now about $0.63h$ for $\mu_L/\mu_0 = 2$, greater than $1.0h$ for $\mu_L/\mu_0 = 4$, and $0.22h$ for $\mu_L/\mu_0 = 8$. The reason for the size for $\mu_L/\mu_0 = 4$ being larger than the size for $\mu_L/\mu_0 = 2$ may be that the stress ratio rises before it reaches the lower bound of 0.9.

We have also studied the K-dominant zone for an interphase model in an interface crack problem. It is assumed that there is an interfacial layer between two dissimilar materials. The model can be obtained by taking the limit $h_T \to \infty$ and keeping h_B fixed in the model of double layered coating with an FGM bottom coat. The FGM bottom coat is now an interfacial layer. Figure 8(a) and (b) shows the stress ratio R_s versus the normalized distance r/h for $h_B/a = 0.1$ and $h_B/a = 0.01$ where h_B is the thickness of the interfacial layer. It is observed that the size of the K-dominant zone decreases with an increase in the ratio, μ_L/μ_0, of the shear moduli of the two dissimilar materials. For $h_B/a = 0.1$, the size of the K-dominant zone is about $0.35h$ for $\mu_L/\mu_0 = 2$, $0.17h$ for $\mu_L/\mu_0 = 4$ and $0.1h$ for $\mu_L/\mu_0 = 8$. For $h_B/a = 0.01$ [see Fig. 8(b)] the size of the K-dominant zone is about $0.45h$ for $\mu_L/\mu_0 = 2$, $0.15h$ for $\mu_L/\mu_0 = 4$ and $0.07h$ for $\mu_L/\mu_0 = 8$. Hence, when the shear moduli of two dissimilar materials differ by a large amount, the interphase layer model may not be valid since there may not exist a K-dominant zone, i.e. the K-dominant zone falls into the crack tip nonlinear deformation and damage zone.

6. CONCLUSIONS

The interface cracking between ceramic and/or FGM coatings and a substrate has been studied under antiplane shear loading conditions. Mode III stress intensity factors at an interface crack tip are calculated for four different coatings, namely: single layered homogeneous coating, double layered piece-wise homogeneous coating, single layered FGM coating and double layered coating with an FGM bottom coat. When the shear modulus of the coating is higher than that of the substrate, it is found that the single layered FGM coating reduces the SIF. However, the coating system with a top homogeneous layer and a thin FGM bottom layer reduces SIF more significantly. When the shear modulus of the coating is lower than that of the substrate, the SIF is found to be larger for the FGM coatings than that for the homogeneous coatings. The FGM coating may still be superior to a homogeneous coating in this case as FGM coatings usually provide better bonding

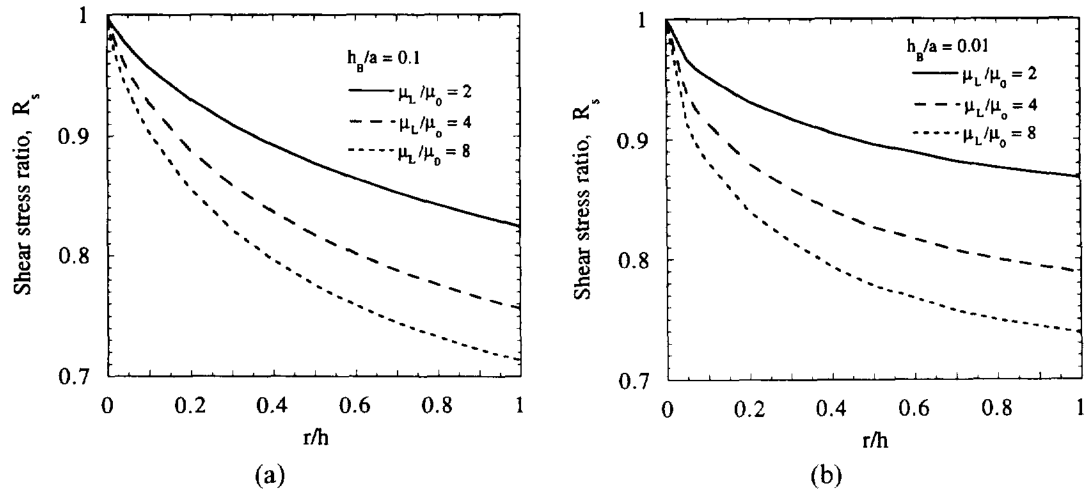

Fig. 8. The square-root singular stress divided by the total stress, $R_s = \tau_y^K/\tau_y$, at the crack extension line ($r = x - a > 0,\ y = 0$) for an interlayer crack: (a) $h_B/a = 0.1$; (b) $h_B/a = 0.01$.

strength between the coating and substrate. Large shear modulus gradients in FGM coatings may seriously restrict the application of the stress intensity factor concept as the size of the K-dominant zone decreases with an increase in the shear modulus differential in the coating and substrate for a fixed coating thickness. The same argument also applies to interphase models in interface crack problems.

We note that the aforestated conclusions arrived at for the antiplane shear loading may not be valid for the more important case of mode I and mode II fracture wherein oscillatory singular stress fields generally exist at the interface crack tip between a homogeneous coating and a substrate.

Acknowledgements— The partial support of this work from the Office of Naval Research under grant number N00014-94-1-1211 with Dr Y. D. S. Rajapakse as program manager is gratefully acknowledged.

REFERENCES

[1] J. A. NESBITT, N. S. JACOBSON and R. A. MILLER, in *Surface Modification Engineering*, Vol. II (Edited by R. KOSSOWSKY), p. 25. CRC Press, Boca Raton, FL (1989).
[2] H. HERMAN, C. C. BERNDT and H. WANG, in *Ceramic Films and Coatings* (Edited by J. B. WACHTMAN and R. A. HABER), p. 131. Noyes Publications, Park Ridge, NJ (1993).
[3] T. E. HALE, in *Ceramic Films and Coatings* (Edited by J. B. WACHTMAN and R. A. HABER), p. 22. Noyes Publications, Park Ridge, NJ (1993).
[4] D. E. Graham, in *Ceramic Cutting Tools* (Edited by E. D. WHITNEY), p. 221. Noyes Publications, Park Ridge, NJ (1994).
[5] Y. KURODA, K. KUSAKA, A. MORO and M. TOGAWA, in *Ceramic Transactions, Vol. 34: Functionally Gradient Materials* (Edited by J. B. HOLT, M. KOIZUMI, T. HIRAI and Z. A. MUNIR), p. 289. American Ceramic Society, Westerville, OH (1993).
[6] H. TAKAHASHI, T. ISHIKAWA, D. OKUGAWA and T. HASHIDA, in *Thermal Shock and Thermal Fatigue Behavior of Advanced Ceramics* (Edited by G. A. SCHNEIDER and G. PETZOW), p. 543. Kluwer Academic Publishers, Dordrecht (1993).
[7] M. KOIZUMI, in *Ceramic Transactions, Vol. 34: Functionally Gradient Materials*, (Edited by J. B. HOLT, M. KOIZUMI, T. HIRAI and Z. A. MUNIR), p. 3. American Ceramic Society, Westerville, OH (1993).
[8] F. ERDOGAN, *Comp. Engng* **5**, 753 (1995).
[9] Z.-H. JIN and N. NODA, *ASME J. Appl. Mech.* **61**, 738 (1994).
[10] Z.-H. JIN and R. C. BATRA, *J. Mech. Phys. Solids* **44**, 1221 (1996).
[11] R. S. DHALIWAL and B. M. SINGH, *J. Elasticity* **8**, 211 (1978).
[12] F. DELALE and F. ERDOGAN, *ASME J. Appl. Mech.* **50**, 609 (1983).
[13] F. ERDOGAN, *ASME J. Appl. Mech.* **52**, 823 (1985).
[14] F. DELALE and F. ERDOGAN, *Int. J. Engng Sci.* **26**, 559 (1988).
[15] M. OZTURK and F. ERDOGAN, *Int. J. Engng Sci.* **31**, 1641 (1993).
[16] N. NODA and Z.-H. JIN, *Int. J. Solids Struct.* **30**, 1039 (1993).
[17] Z.-H. JIN and N. NODA, *Int. J. Solids Struct.* **31**, 203 (1994).
[18] G. BAO and L. WANG, *Int. J. Solids Struct.* **32**, 2853 (1995).
[19] F. ERDOGAN and M. OZTURK, *Int. J. Engng Sci.* **33**, 2179 (1995).

[20] N. I. MUSKHELISHVILI, *Singular Integral Equations.* Noordhoff, Groningen (1965).
[21] F. ERDOGAN, G. D. GUPTA and T. S. COOK, in *Mechanics of Fracture*, Vol. 1 (Edited by G. C. SIH), p. 368. Noordhoff International Publishing, Leyden (1973).
[22] C. ATKINSON, *Int. J. Fracture* **13,** 807 (1977).
[23] F. DELALE and F. ERDOGAN, *ASME J. Appl. Mech.* **55,** 317 (1988).
[24] W. YANG and C. F. SHIH, *Int. J. Solids Struct.* **31,** 985 (1994).

(Received 27 March 1996; accepted 13 May 1996)